Permeability Calculation in a Fracture Network - 12197

Cheo Kyung Lee *, Hyo Won Kim*,
Sung Paal Yim **
* Handong Global University,
3 Namsong-ri, Heunghae-eub, Buk-gu, Pohang, Kyungbuk, 791-708
Republic of Korea
** Korea Atomic Energy Research Institute,
Yusong, Daejon, 305-600
Republic of Korea

ABSTRACT

Laminar flow of a viscous fluid in the pore space of a saturated fractured rock medium is considered to
calculate the effective permeability of the medium. The effective permeability is determined from the flow field which is calculated numerically by using the finite element method. The computation of permeability components is carried out with a few different discretizations for a number of fracture arrangements. Various features such as flow field in the fracture channels, the convergence of permeability, and the variation of permeability among different fracture networks are discussed. The longitudinal permeability in general appears greater than the transverse ones. The former shows minor variations with fracture arrangement whereas the latter appears to be more sensitive to the arrangement

INTRODUCTION

Fracture networks are commonly observed in the underground rock media. Under pressure anomaly in a water-saturated medium, fluid flow takes place and it significantly influences the transport of solute in water. The fluid flow pattern depends on not only the externally imposed pressure gradient but also the fracture arrangement in the network.

The characteristics of the flow through a porous medium are usually discussed with the effective permeability of the medium. Therefore it is of utmost importance to evaluate the permeability from accurate description of the flow field inside the fracture channels. It is also very important for effective management of the underground repository located in a rock medium with fracture network.

In this study, the process of fluid flow through a medium with fracture network on the microscale is investigated with emphasis on the effective macroscale permeability coefficient.

The theoretical framework is based on the homogenization theory which systematically combines the processes on the microscale and deduces the governing equations and the effective coefficients on the macroscale[1]. Under two basic assumptions, (i) the periodicity of the medium structure on the microscale with periodic length *l* and (ii) the periodicity of all variables and material properties with the same periodic length. The periodicity assumption is not very restrictive because the distributions and arrangements over the periodic length are quite arbitrary.

The fracture network used in the present study is composed of four fractures. This is a continuation of the effort in a similar work for a fracture network composed of three fractures[2]. Two fractures are parallel to each other and are aligned along the direction of 45-deg

counterclockwise from the horizontal direction. The third and fourth ones connect the parallel fractures at different angles. Specifically three cases are considered: (i) the spacing between the connecting fractures decreases when moving from the lower parallel one to the upper parallel one (narrowing), (ii) the spacing between the connecting fractures is constant and they are normal to the parallel fractures(parallel), and (iii) the spacing between the connecting fractures increases when moving from the lower parallel one to the upper parallel one(widening).

The longitudinal permeability(permeability in the same direction as the externally-imposed pressure gradient) generally appears to be greater than the transverse one(permeability in the direction normal to the external pressure gradient), as can be expected for most medium structure, and is rather insensitive to the inclination pattern of the connecting fractures. On the other hand, the transverse permeability, which is smaller than the longitudinal one, appears to be affected much more by the connecting fracture inclination even though the differences in the inclination pattern are minor.

Various features including flow field distribution in the fracture channels, the convergence of permeability, and the variation of permeability among different fracture networks are discussed.

MULTIPLE SCALE ANALYSIS

The features of the multiple scale perturbation analysis used in [2] are briefly reproduced. Recognizing the scale disparity in the process of fluid flow, two distinct length scales are introduced: the microscale(the fast scale which is equivalent to the size of the representative elementary volume in the traditional treatment of the problem) and the macroscale(the scale over which the process of interest takes place from the viewpoint of reservoir engineering and management).

The variables are expanded as perturbation series by using the following small parameter:

$$\frac{\ell}{\ell'} = \epsilon \ll 1$$

in which *l* is the microscale length and *l′* is the macroscale length. Upon expansion of the governing equations and boundary conditions, the microscale boundary-value problems are investigated separately according to the respective order of ϵ and, via volume-averaging over the micro-cell with the size *l*, the macroscale governing equations and the effective coefficients are derived.

In the process of the multiple scale analysis, a canonical micro-cell boundary-value problem is defined whose solution is used in the calculation of the effective permeability of the medium by averaging over the micro-cell volume.

THE MICRO-CELL BOUNDARY-VALUE PROBLEMS

For fluid flow the following Stokes problems is defined:

$$\begin{aligned}
\nabla^2\mathbf{K} - \nabla\mathbf{S} + \mathbf{I} &= 0 \quad \text{in} \quad \Omega_f \\
\nabla\cdot\mathbf{K} &= 0 \quad \text{in} \quad \Omega_f \\
\mathbf{K} &= 0 \quad \text{on} \quad \Gamma \\
\langle\mathbf{S}\rangle &= 0 \\
\mathbf{K} \text{ and } \mathbf{S} \text{ are } &\ \Omega- \text{ periodic.}
\end{aligned} \tag{1a-e}$$

In the above, **K=**K_{ij} and **S=**S_j are the fluid velocity in the i-th direction and the fluid pressure in the micro-cell due to externally imposed pressure gradient in the j-th direction.

The macroscale permeability is then given by the micro-cell volume average of **K** as

$$\langle \mathbf{K} \rangle = \frac{1}{\Omega} \int_{\Omega} \mathbf{K} d\Omega \tag{2}$$

and the Darcy's law is given as

$$\langle \mathbf{v}^{(0)} \rangle = -\langle \mathbf{K} \rangle \cdot \nabla' p^{(0)} \tag{3}$$

where the left-hand side is the seepage velocity and the primed gradient is the derivative of the fluid pressure over the macroscale. This serves as the momentum equation on the macroscale.

THE FRACTURE GEOMETRIES

The geometries of fracture network used in the present study to calculate the permeability are shown in Fig. 1 (a) – (c).

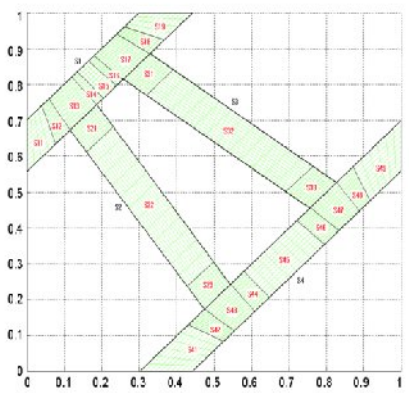

(a)

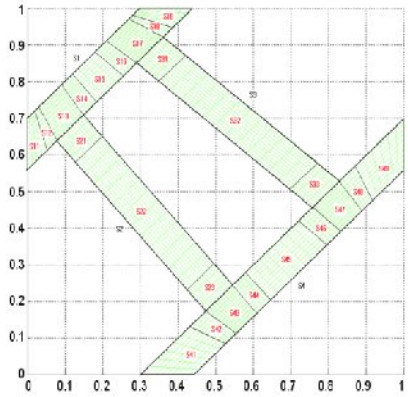

(b)

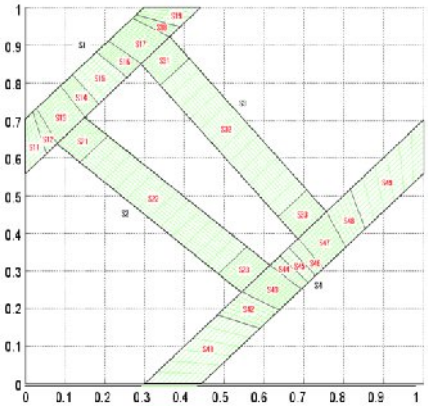

(c)

Fig. 1. Three different types of fracture network: (a) Narrowing, (b) Parallel, and (c) Widening. The macroscale pressure gradient is in the horizontal(x-) direction.

NUMERICAL CALCULATION

The direction of the externally imposed macroscale pressure gradient is chosen to be in the horizontal(x-) direction for the fracture geometries sown in Fig. 1.

Discretization

For each of the cases (i), (ii) and (iii), three different meshes have been used and are summarized in Table I below in which Ne is the total number of elements used in the numerical calculation of the flow field in the fracture. Specifically increasing Ne indicates refined discretizations in the blocks near the junctions of fractures in Fig. 1.

Table I. Discretization of the fracture channel

Case (i)

	Case (i)-1	Case (i)-2	Case (i)-3
Ne	780	1016	1296

Case (ii)

	Case (ii)-1	Case (ii)-2	Case (ii)-3
Ne	780	1016	1296

Case (iii)

	Case (iii)-1	Case (iii)-2	Case (iii)-3
Ne	780	1016	1296

Flow field in the fracture network

The results of the calculated flow field for Cases (i), (ii) and (iii) are shown in Figs. 2-4.

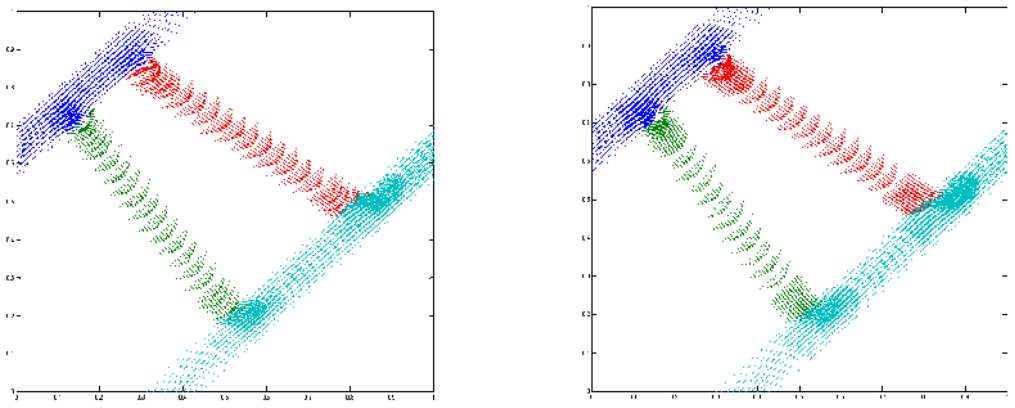

(a) (b)

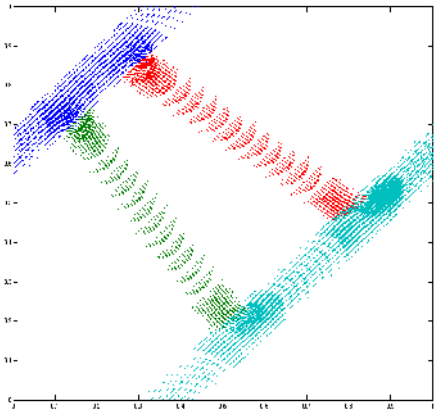

(c)

Fig. 2. Flow field for the case (i) of narrowing connecting channels with different discretization: (a) Case (i)-1, (b) Case (i)-2, and (c) Case (i)-3. The number of elements increases from (a) to (c) as summarized in Table I.

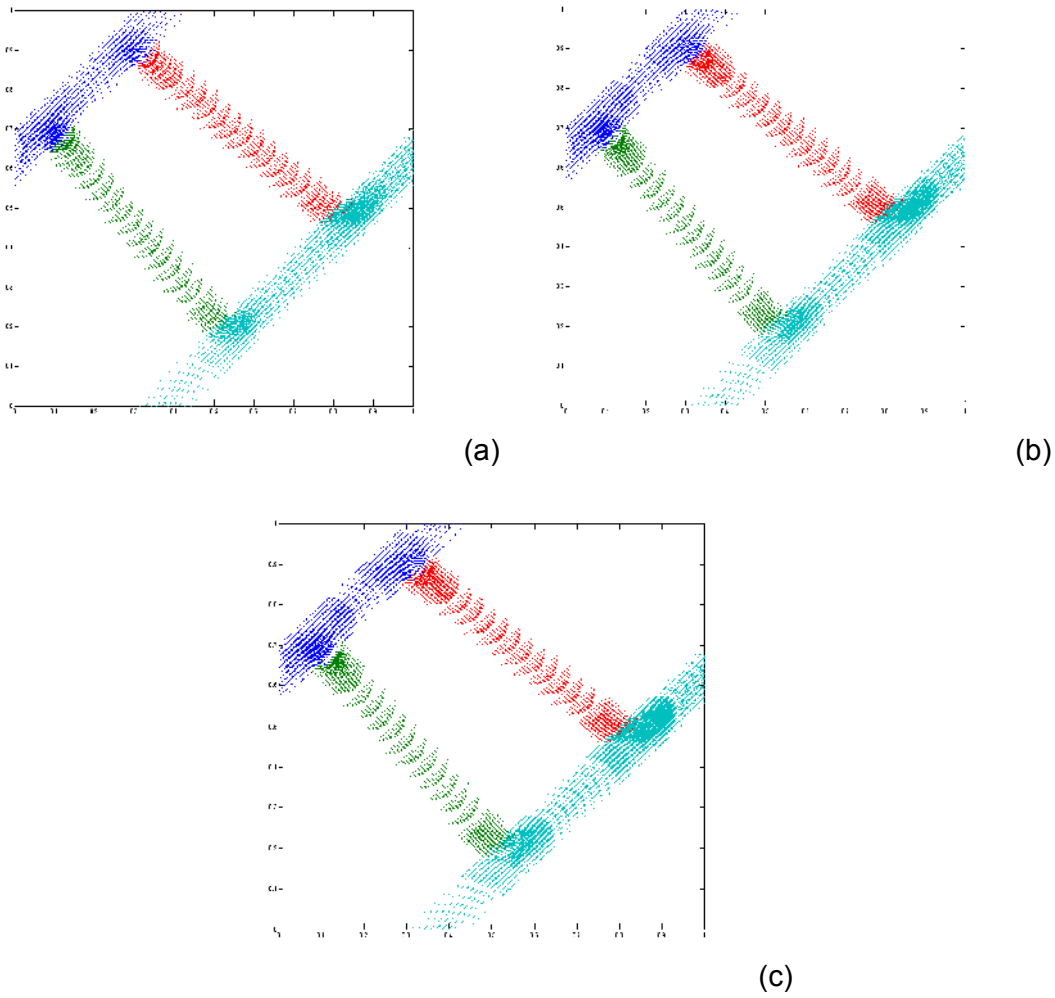

Fig. 3. Flow field for the case (ii) of parallel connecting channels with different discretization: (a) Case (ii)-1, (b) Case (ii)-2, and (c) Case (ii)-3. The number of elements increases from (a) to (c) as summarized in Table I.

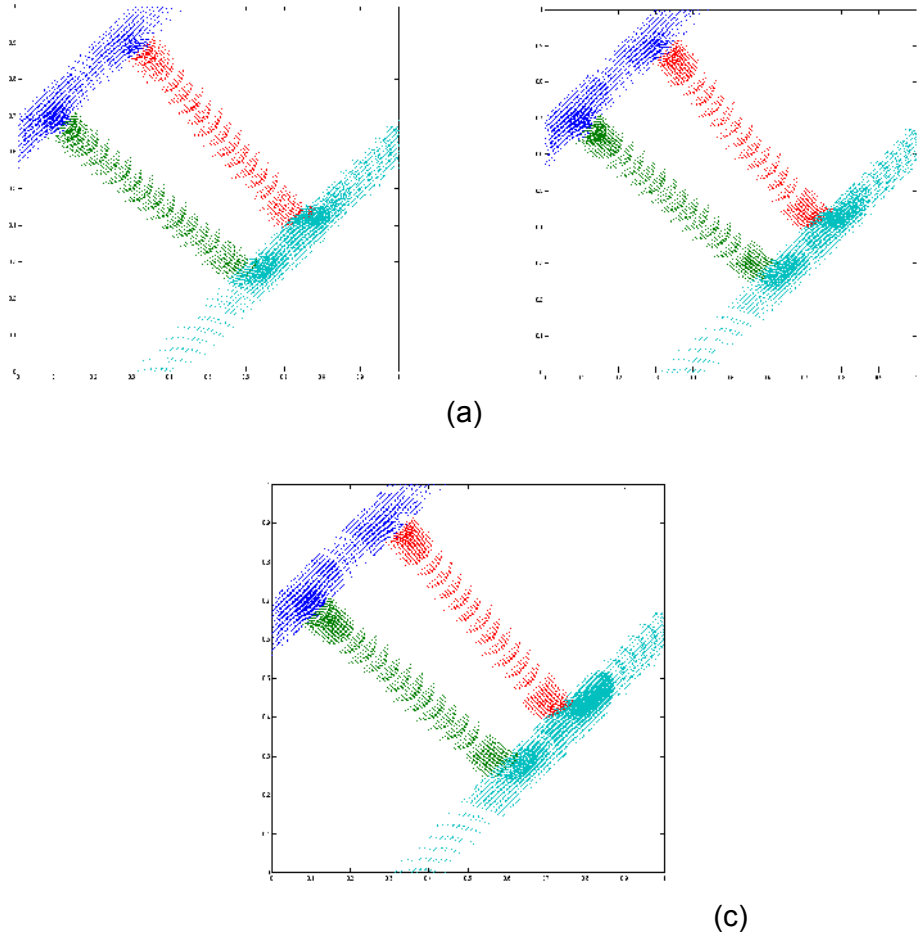

Fig. 4. Flow field for the case (ii) of widening connecting channels with different discretization: (a) Case (iii)-1, (b) Case (iii)-2, and (c) Case (iii)-3. The number of elements increases from (a) to (c) as summarized in Table I.

As mentioned earlier, the discretization has been refined around the junctions where the flow field varies most significantly.

RESULTS AND DISCUSSION

The micro-cell boundary-value problem defined above, i.e., the Stokes problem for flow field, was solved by using two-dimensional finite elements. The details are omitted.

The effective permeability on the macroscale has been calculated by volume-averaging of the velocity field over the microcell. The results are summarized in Table II and the errors associated with progressively finer meshes are summarized in Table III. Note that <Kxx> and <Kyx> are the permeability in the x- and y-directions due to an externally imposed pressure gradient in the x-direction respectively.

Table II. Calculated permeability.

	Case 1-1	Case 1-2	Case 1-3

$<K_{xx}>$	1.02633270e-04	1.00302671e-04	9.88649253e-05
$<K_{ux}>$	1.95211556e-05	2.43763746e-05	2.48362424e-05

	Case 2-1	Case 2-2	Case 2-3
$<K_{xx}>$	1.05121946e-04	1.04668866e-04	1.04474120e-04
$<K_{ux}>$	1.23697749e-05	1.78413330e-05	1.78308790e-05

	Case 3-1	Case 3-2	Case 3-3
$<K_{xx}>$	1.01430297e-04	1.01082366e-04	1.00796504e-04
$<K_{ux}>$	1.35370092e-05	2.01847758e-05	2.00679087e-05

Table III. Errors in the calculation of effective permeability..

Error(%)	Case (i)-1 ⟶ Case (i)-2	Case (i)-2 ⟶ Case (i)-3
$<K_{xx}>$	2.24	1.4
$<K_{ux}>$	24.9	1.9

Error(%)	Case (ii)-1 ⟶ Case (ii)-2	Case (ii)-2 ⟶ Case (ii)-3
$<K_{xx}>$	0.38	0.19
$<K_{ux}>$	44.2	0.05

Error(%)	Case (iii)-1 ⟶ Case (iii)-2	Case (iii)-2 ⟶ Case (iii)-3
$<K_{xx}>$	0.39	0.30
$<K_{ux}>$	49	0.55

As shown in Table II, the effective permeability values in the longitudinal direction are greater than the transverse ones which is natural unless the fracture arrangement is such that the transport of the fluid is mostly in the transverse direction by peculiar arrangement of fractures. It is noted from Table III that the convergence becomes much better when moving from the second mesh to the third mesh. The convergence appears to be quite satisfactory and no further refined calculations have been made.

The longitudinal permeability <Kxx> for the parallel connecting fractures[Case (ii)] is larger than those for the narrowing[Case (i)] and the widening[Case (iii)] fractures. For the parallel case the connecting fractures contribute equally to the transport of the fluid from the upper inclined parallel fracture to the lower inclined parallel one. On the other hand, the left connecting fracture in the narrowing case and the right fracture in the widening case tend to reduce fluid transport from the upper inclined parallel fracture to the lower inclined parallel one. As a result, the net

movement of the fluid in the longitudinal direction is decreased thereby resulting in lower permeability.

The transverse permeability <Kyx> is about 20 to 25% of the longitudinal permeability. Specifically <Kyx> for the parallel connecting fractures[Case (ii)] is less than those for Cases (i) and (iii). It is again due to the arrangement of the connecting fractures. Those connecting fractures mentioned above in the discussion of the longitudinal permeability, on the contrary, serve as more efficient passage of the fluid into the transverse direction. As a result, <Kyx> becomes larger in Cases (i) and (iii).

CONCLUSIONS

From the calculations of the permeability in a rock medium with a fracture network(two parallel fractures aligned in the direction of 45-deg counterclockwise from the horizontal and two connecting fractures(narrowing, parallel and widening) the following conclusions are drawn.

1. The permeability of fractured medium not only depends on the primary orientation of the main fractures but also is noticeably influenced by the connecting fractures in the medium.

2. The transverse permeability(the permeability in the direction normal to the direction of the externally imposed macroscale pressure gradient) is only a fraction of the longitudinal one, but is sensitive to the arrangement of the connecting fractures.

3. It is important to figure out the pattern of the fractures that connect(or cross) the main fractures for reliable calculation of the transverse permeability.

ACKNOWLEDGEMENT

This research was supported by Basic Science Research Program through the National Research Foundation of Korea(NRF) funded by the Ministry of Education, Science and Technology(2010-0004808).

REFERENCE

1. C.K. LEE, M.Z. Htway, H.W. and S. P. YIM, “Calculation of Permeability and Dispersion Coefficients in Unsaturated Porous Media with Fractures” ,WM2010, Phoenix, March 7-11(2010)
2. C.K. LEE, M.Z. Htway, H.W. and S. P. YIM, “Permeability and Dispersion Coefficients in Rocks with Fracture Network”, WM2011, Phoenix, Feb. 27 – Mar. 3(2011).